Fast Ion Transport Phenomena in Oriented Semicrystalline LiI−P(EO)$_n$-Based Polymer Electrolytes

D. Golodnitsky,*,†,‡ E. Livshits,† A. Ulus,† Z. Barkay,‡ I. Lapides,§ E. Peled,† S. H. Chung,|| and S. Greenbaum||

School of Chemistry, Tel Aviv University, Wolfson Applied Materials Research Center, Tel Aviv 69978, Israel, Department of Analytical Chemistry, Hebrew University, Jerusalem, Israel, and Physics Department, Hunter College of CUNY, New York, New York 10021

Received: July 5, 2001

We have employed a variety of experimental methods, including DC and AC conductivity, scanning electron microscopy (SEM), atomic force microscopy (AFM), differential scanning calorimetry (DSC), Fourier Transform Infrared (FTIR) spectroscopy, and pulsed field gradient nuclear magnetic resonance (NMR), to investigate the poly(ethylene oxide):LiI system. The effect of stretching the polymer electrolyte on its DC conductivity is dramatic, resulting in up to a 40-fold increase in the LiI P(EO)$_7$ composition. Structural ordering imposed by the stretching is observed in SEM and AFM images, and the cation solvation sheath (i.e., the helical PEO structure) is also affected by stretching in a manner believed to favor enhanced transport, according to the FTIR results. The NMR results demonstrate unambiguously that Li^+ diffusivity is anisotropic and enhanced along the stretch direction. Although the cation transport mechanism in polyether−salt polymer electrolytes is believed to rely heavily on polymer segmental mobility, this investigation suggests that other factors also contribute significantly. Such factors which can be augmented by stretching are modest changes in the cation solvation sheath and alignment of the helical structural units characteristic of PEO and its salt complexes.

Introduction

The growing attention to the ion-conducting polymers is mainly a result of the development of high quality processable and environmentally stable materials for use in areas such as rechargeable batteries, electrochromic devices, and sensors. Moreover, polymer electrolytes are of theoretical interest as model materials for the investigation of conduction paths in semicrystalline (partially ordered) systems.

The main distinction between ion transport in low-molecular-weight liquid solvents and in high-molecular-weight solid polymers is that ion transport in the latter is decoupled from the macroscopic viscosity of the electrolyte. This is because the polymer chains are entangled and cannot move over long distances with the ion. However, ion transport is intimately linked to the microscopic viscosity of short segments of the polymer chains. Therefore, most of the research on new polymer electrolytes (PE) has been guided by the principle that ion transport is strongly dependent on local motion of the polymer in the vicinity of the ion.[1−5] A thorough review of theoretical treatments for conductivity processes was published by Ratner.[6] Ions are thought to be transported by quasi-random motion of short polymer segments and the conductivity is generally observed to rise with increasing flexibility of the polymer chains. According to the dynamic bond percolation theory (DBP) proposed by Druger et al.[7] for conductivity in dilute polymer electrolytes, cation and anion motions are considered to be fundamentally different. Cation motion is visualized as the making and breaking of coordinate bonds with motion between coordinating sites, while anion motion is regarded as a hopping between an occupied site and a void large enough to contain the ion. The scale time for ion motions is of the same order as for polymer relaxation, thus ion transport depends on the relaxation dynamics of the polymer host.

Polymer−salt complexes of poly(ethylene oxide) (PEO) and other polymer hosts can have a high degree of crystallinity and these crystalline phases represent well-defined stoichiometric structures. Depending on the composition and temperature these systems also contain either the pure crystalline polymer or an amorphous phase and may be described by pseudophase diagrams.[8−10] The crystal structures of alkali metal complexes with PEO reveal that for all ion sizes from Li^+ to K^+ the cations are accommodated within the PEO helix. In the case of lithium triflate ($LiCF_3SO_3$), Li^+ is five-coordinate joined to three ether oxygens and one oxygen from each of two triflate groups. There is a lithium ion in each turn of the helix. In the case of PEO_4:MSCN, where M = K^+, NH_4^+, or Rb^+, the cations are seven-coordinate (five ether oxygens and two nitrogens from the thiocyanate anions). Rb^+ and Cs^+ form amorphous PEO complexes in contrast with highly crystalline lithium, sodium, and potassium−PEO electrolytes.[11]

The recognition that cations are enclosed within the PEO helices suggests the possibility that cation transport may occur efficiently along the helical axis. This idea was originally proposed by Armand[12] over two decades ago, and the more recent structural refinements of Bruce and co-workers[13] also suggest a helical pathway for the cations. The five- to 20-fold stretching-induced conductivity enhancement in the axial force direction of the highly oriented LiI−P(EO)$_{20}$ polymer electro-

* Corresponding author. E-mail:golod@post.tau.ac.il.
† Tel Aviv University.
‡ Wolfson Applied Materials Research Center.
§ Hebrew University.
|| Hunter College of CUNY.

10.1021/jp012547l CCC: $20.00
Published on Web 10/16/2001

lyte, originally found by us,[14−16] establishes the possibility of interhelical ion motion. Similar ion-transport mechanisms are known in other contexts. For example, cations such as K^+ are known to be transported through channeled structures in biological systems.[17] The evidence of anisotropic transport of the widely used drug digoxin, mediated by human P-glycoprotein, was reported in ref 18. However, this type of channeled transport will be effective for finite distances that will not be sufficient to account for bulk ionic conductivity. Its relative contribution to the overall ionic conductivity will increase under suitable conditions, such as alignment of the chains, and may make it possible for long-range ion conduction to take place independently of large-scale segmental relaxation.

In this study, we attempt to further elucidate the complex interplay between ionic transport processes and macroscopic order. The effect of uniaxial stress on the polymer electrolyte long- and short-range structures is investigated in dilute and concentrated LiI:P(EO)$_n$ ($3 \leq n \leq 100$) PEs. The correlation between ionic transport and the distribution of molecular orientations in solid polymer electrolytes will be studied.

Experimental Section

The electrolytes were prepared from poly(ethylene oxide) (P(EO)) (Aldrich, average molar mass 5×10^6), which was vacuum-dried at 45 to 50° C for about 24 h. The LiI (Aldrich) was vacuum-dried at 150° C for about 24 h. All subsequent handling of these materials took place under an argon atmosphere in a VAC glovebox with water content < 10 ppm. The thickness of the solvent-free films was 150 μm. The films were cut, hot pressed together with the incorporated four 0.05 mm-thick wire electrodes as shown in refs 14−16. Experimental details of the PE preparation and stretching is described elsewhere.[14−16] The lengthwise conductivity measurements during stretching were performed with a homemade system in the galvanostatic mode with the use of four electrodes.[14−16] Four-probe-dc in-situ measurements were carried out in the ordinary way, namely, the voltage drop was measured on a known resistance of 8 MΩ and the calculated current was used to extract the unknown polymer electrolyte resistance from the measurement of the voltage drop between two internal electrodes. The voltage measurements were taken every 30 s under extending lengthwise load.

The AC conductivity in the perpendicular direction was measured ex-situ with the use of a Solartron 1255 frequency-response analyzer controlled by a 586 PC in the frequency range 1 MHz−1 Hz. The polymer electrolyte sample of 1 cm^2 area was placed between two lithium electrodes under a spring pressure of 49 N/cm^2. The configuration of the cell is described in ref 19. The accuracy of the calculation of bulk resistance (R_b) is estimated to be about ±10%.

A JSM-6300 scanning microscope (JEOL Co.) equipped with a Link elemental analyzer and a silicon detector was used for a surface morphology study. The atomic force microscope (AFM) images were obtained in NC (Non-Contact) mode using the Autoprobe M5 system of Thermomicroscopes. The probe was a silicon cantilever with a silicon conical tip of high aspect ratio, having a 3N/m force constant and 90 kHz resonant frequency. Noncontact operation was chosen to reduce the contact forces between the probe and the sample, while scanning at a height of about 30 nm above the surface. The nonflatness of the samples and the instrument few micron *z*-movement actually limited the available maximum scan size to about 20 μm. The scan size of the samples thus varied in the range of 0.5 to 20 μm.

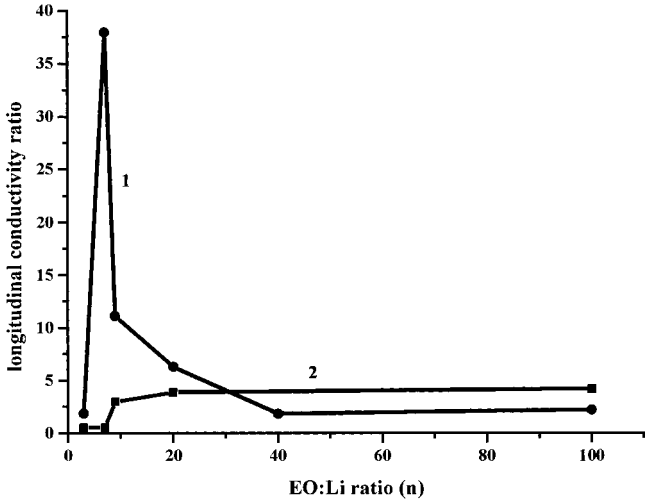

Figure 1. Effect of hot (65 °C) stretching (1) and temperature increase from 28 to 60 °C (2) on the DC conductivity change vs Li:EO ratio in LiI:P(EO)$_n$ electrolyte along the stretch direction.

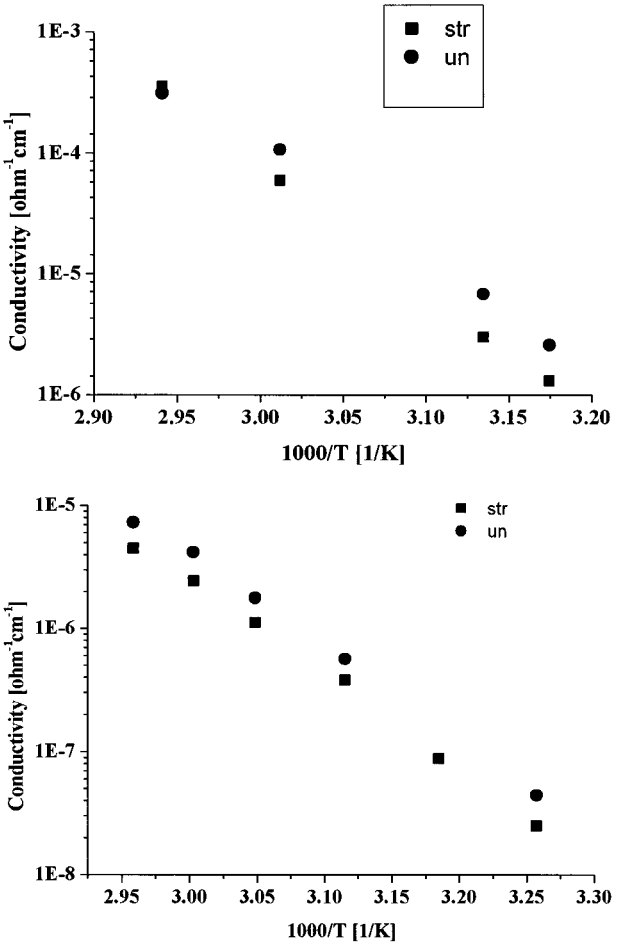

Figure 2. Arrhenius plot of the LiI−P(EO)$_{20}$ (a) and LiI−P(EO)$_7$ (b) polymer electrolyte: AC conductivity measured in the perpendicular direction.

The DSC tests were carried out with TA Instruments module 2010 and System Controller 2100. DSC runs were recorded at a scan rate of 10 deg/min up to 200 °C. A liquid nitrogen cooling accessory was used for subambient temperature tests. FTIR spectra polymer films were recorded by a Bruker IFS 113v FTIR Spectrophotometer. The samples were placed between two KBr standard size disks in inert atmosphere.

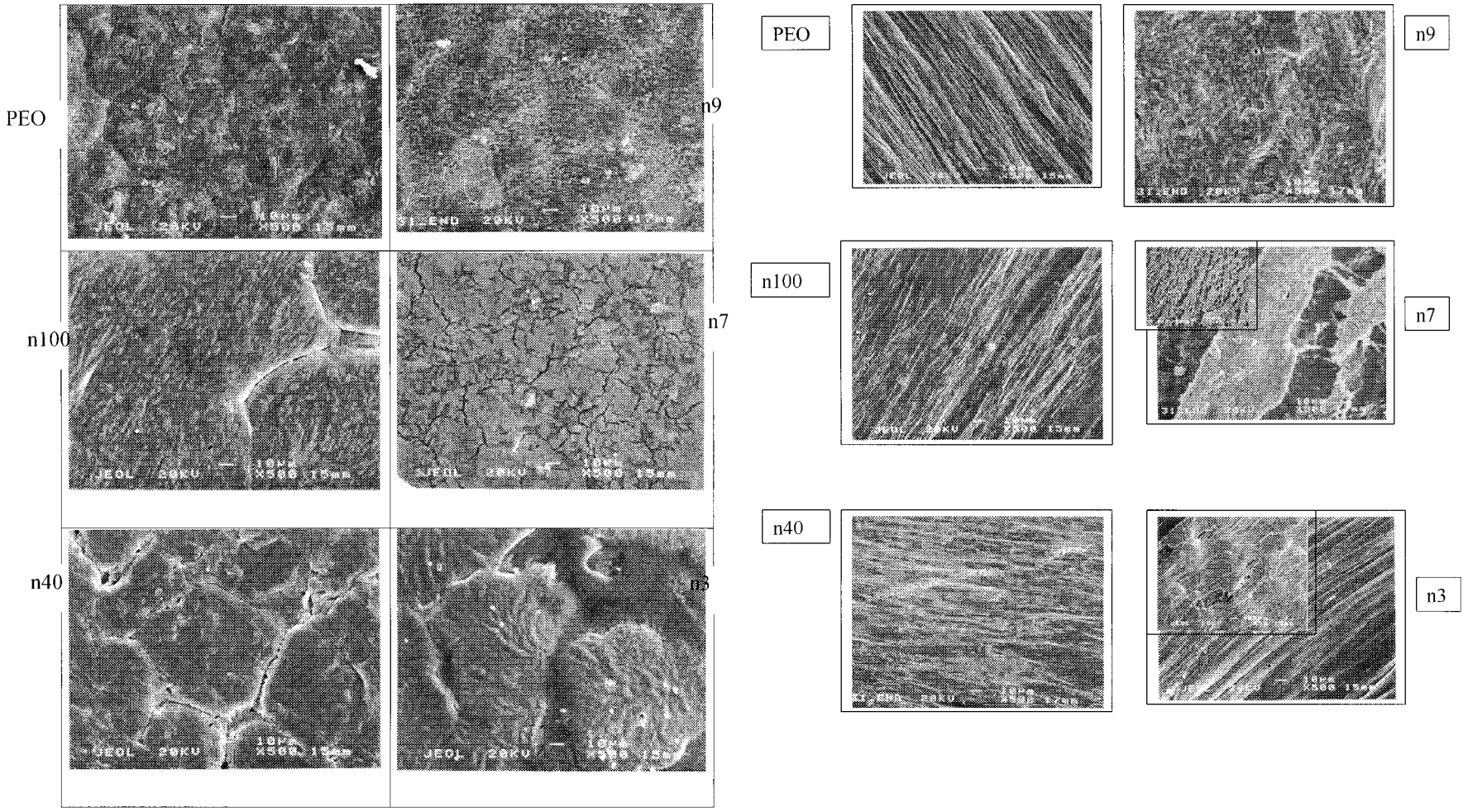

Figure 3. (a) SEM micrographs of unstretched LiI:P(EO)$_n$ polymer electrolytes. (b) SEM micrographs of hot (65 °C)-stretched LiI:P(EO)$_n$ polymer electrolytes.

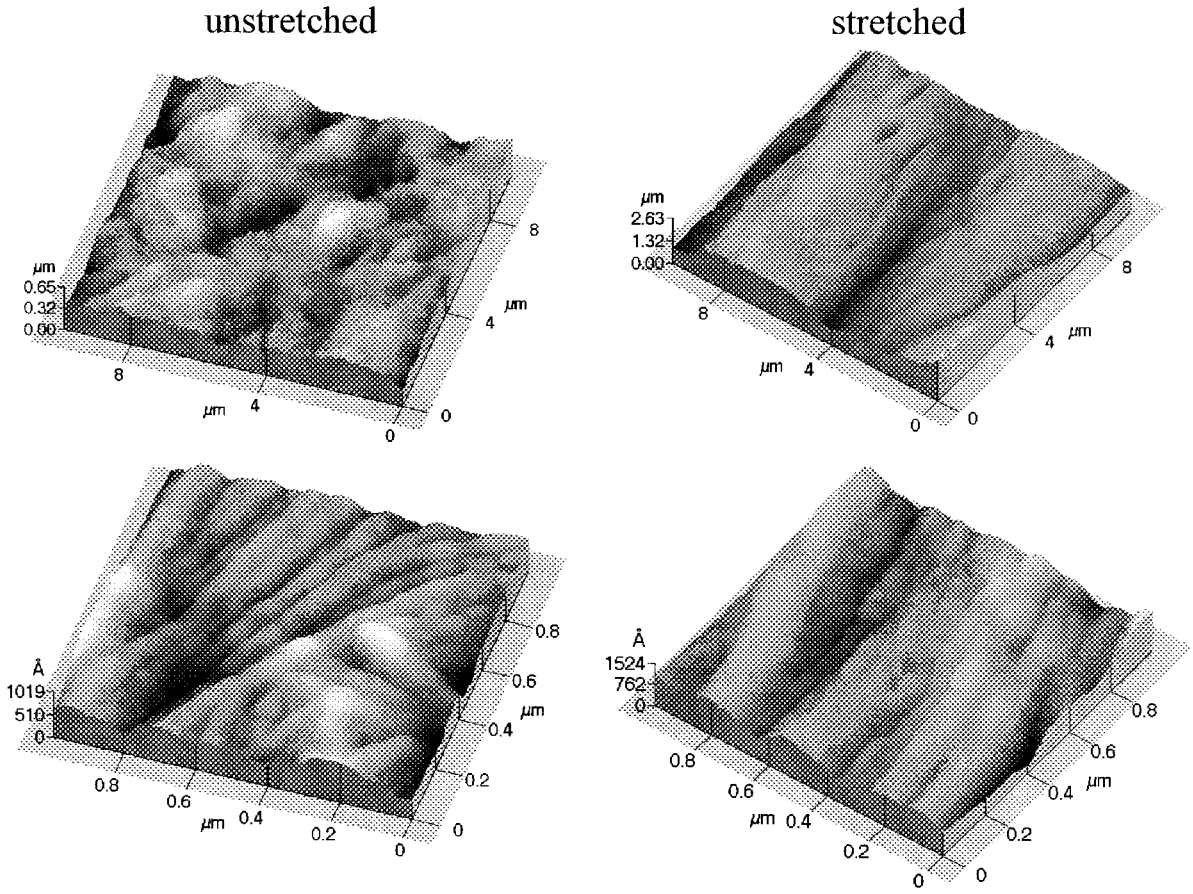

Figure 4. Three-dimensional AFM images of LiI:P(EO)$_{40}$ polymer electrolyte.

NMR measurements were conducted on a Chemagnetics CMX300 Spectrometer operating at a ^{7}Li resonance frequency of 117.0 MHz. Spectra were obtained by collecting the free induction decay (FID) following a single $\pi/2$ pulse (4 μs) and Fourier transforming the data. Details regarding the pulse gradient spin−echo (PGSE) NMR experiments are described elsewhere.[20] The NMR diffusion measurement uses the Hahn spin−echo pulse sequence with a pair of square-shaped gradient field pulses of magnitude g and duration δ. The echo amplitude

$$A(g) = \exp[-\gamma^2 D g^2 \delta^2 (\Delta - \delta/3)] \qquad (1)$$

is attenuated by an amount dependent on how much the position of the spins has changed by the process of self-diffusion D in the time interval Δ and for a series of gradient strengths g = 0.2−1.2 T/m. Spectral and PGSE measurements were performed for the 1:7 and 1:9 samples. However no attenuation of the ^{7}Li signal could be observed for the 1:7 sample at all temperatures. To test for possible anisotropy in the diffusion coefficient, measurements were made on a single piece of the stretched or unstretched 1:9 sample at two angular orientations where the stretch direction is parallel and orthogonal to the static magnetic field B_o. Measurements were made at 60 °C because the spin−echo signal exhibited negligible decay at room temperature, due to a combination of short spin−spin relaxation time and low diffusion rate. Reported values for self-diffusion coefficients are subject to a ±10% uncertainty. We also checked for angular dependence of the spin−lattice relaxation time T_1 but did not find any orientation dependence.

Results and Discussion

The experimental data of the in-situ longitudinal DC conductivity measurements of dilute and concentrated LiI P(EO)$_n$ polymer electrolytes are shown in Figure 1. Temperature increase from the room temperature to about the melting point of the PEO is followed by almost 5-fold conductivity rise of dilute electrolytes. No significant changes were detected for concentrated systems. The stretching process was found to influence the DC conductivity in the direction of the applied force more strongly than does an increase in temperature from 28° to 60 °C. The maximal conductivity enhancement (about 40-fold) in the direction of applied force was achieved in the LiI P(EO)$_7$ electrolyte with highly elastic rubber-like structure. It should be mentioned that the absolute σ_{DC} value at room temperature approaches 0.1 mS/cm.

The room-temperature AC conductivity (σ_{AC}) of the stretched LiI−P(EO)$_{20}$ and LiI−P(EO)$_7$ electrolytes measured in the perpendicular direction was about half the values in the unstretched film. Close to the melting point of the PEO the perpendicular σ_{AC} values of the stretched polymer electrolytes with n = 20 approach those of the unstretched. At n = 7, however, the difference in the perpendicular σ_{AC} remains (Figure 2). It is noteworthy that at n = 20 and T below 45 °C the apparent activation energy of conduction in the axial direction of the stretched PE is 10 to 50 times smaller than that of the perpendicular direction. Although direct comparison between DC conductivities in the parallel and perpendicular orientations would obviously be most relevant, the geometric constraints associated with the experimental setup did not allow for this.

Figure 3a shows SEM micrographs of LiI−P(EO)$_n$ unstretched films with 100 ≥ n ≥ 3. All the samples exhibit grain crystalline structure. The grain size varies from 100 to 150 μm, except for PE with n = 7, the grains of which are smaller and do not exceed 50 μm. Hot (65 °C) stretching of dilute PEs, which results in their flowing (plastic deformation), is followed

by the formation of unidirectionally oriented fiberlike microphases of several micron width as shown in Figure 3b. The critical flowing force depends on the salt concentration and varies from 450 to 850 N/cm^2. The stretched LiI−P(EO)$_7$ polymer electrolyte, not like the other PEs, has highly elastic rubber structure, the relaxation of which starts immediately after release of the load. To achieve nonreversible structural changes the film of LiI−P(EO)$_7$ electrolyte was kept under the load at about 65 °C for at least 12 h. As can be seen from Figure 3b, aligned oriented regions of the polymer electrolyte with $n = 7$ are of several tenths of a micron width. The LiI−P(EO)$_9$ polymer electrolyte behaves similarly on stretching; its rubber properties, however, are less pronounced. Highly concentrated PEs with $n = 3$ were stretched partially as they tend to break and not to flow.

Three-dimensional topography images of unstretched LiI P(EO)$_{40}$ polymer electrolyte were taken with the use of AFM. It is clear that the sample consists of several micron-size randomly oriented separate domains, as shown in Figure 4a. Each domain is composed of either partially aligned or entangled fibers. Upon stretching, the large separate units as well as fibers gain a preferred orientation as suggested in Figure 4b. The width of the fibers, estimated from the height profile, varied from 40 to 80 nm. This is in agreement with the size of crystalline microphases calculated from X-ray diffraction data.[21] The average diameter of the individual fibers is about 40−50 Å. We believe that each fiber, in turn, contains several helical PEO macromolecules. It it suggested that there are at least three degrees of stretching-induced structural long- and short-range order.

DSC examination of the unstretched PEs (Figure 5) shows that with the decrease in n from 100 to 7 the glass transition temperature (T_g) increases from −32.7 to −1 °C in agreement with data published for other PEO-based electrolytes.[1−4] Onset temperature (T_{on}) of the first melting transition (58 °C) is almost invariant for PEs for dilute electrolytes. At an EO:Li ratio of 9, two melting peaks are distinguished and T_{on} of the first peak is 55.4 °C. The enthalpy of the melting peaks decreases with increasing n from 145 to 80 J/g, in agreement with reduced amount of the crystalline phase of the pure PEO. When the films are stretched the T_g vs n dependence is reversed; that is, the value of T_g of dilute PEs with $n > 20$ is higher than that of rubber-like structure electrolytes ($n = 7$ and 9). In dilute polymer electrolytes the positive shift of T_g as a result of stretching is extremely strong (up to about 30 K), while in stretched LiI P(EO)$_9$ this shift is 6 K only. The onset temperature of the melting peak of stretched dilute PEs increases by 2.5 to 4 K. The endothermic peaks of melting of dilute polymer electrolytes become narrower as a result of stretching. This is followed by an increase in their height from 30 to 60%, indicating that stretching increases the structural order of the polymer electrolyte. The intensity of the low-temperature melting transition of the stretched LiI P(EO)$_9$ electrolyte, which can be assigned to the melting of a eutectic, dramatically increases on stretching, while the second (liquidus) peak becomes scarcely visible. A cold crystallization peak appears in the DSC run of the stretched LiI P(EO)$_9$ PE, indicating a large degree of metastability.

It is well established that ion motion is not simply the diffusion of a single ion or ion cluster, but rather involves formation of different coordination environments around the mobile ions. IR spectroscopy is an effective tool to examine such conformational changes. Six main regions of the IR peaks (below 600, at 900−800, ∼1340, ∼1460, ∼2000, and 3600−2600 cm^{-1}) have been identified in the IR spectra of LiI−P(EO)$_n$

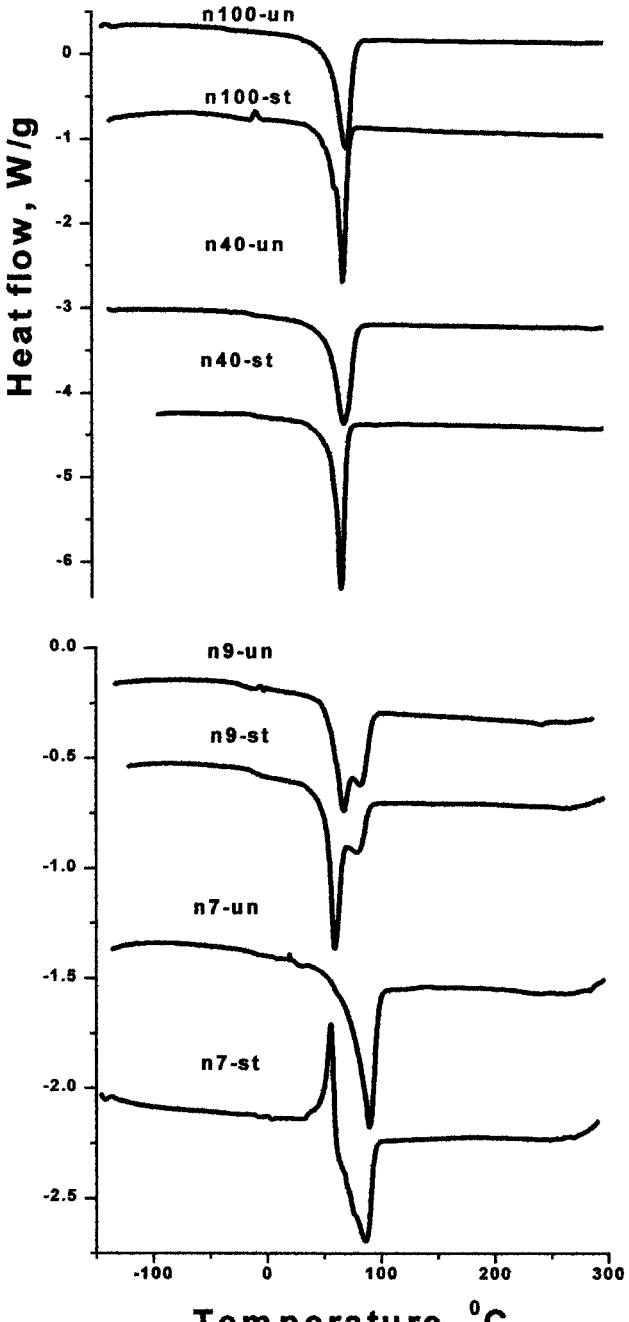

Figure 5. Differential scanning calorimetry (DSC) thermograms of various LiI:P(EO)$_n$ polymer electrolytes, with n-values indicated; un: unstretched, st: stretched.

polymer electrolytes.[21] Most of the bands were found to be sensitive to changes in LiI concentration and to stretching of polymer electrolytes. IR spectra of the salt−PEO complex appear to be a superposition of the pure PEO spectrum and additional bands, which can be attributed to the 1:3 complex.

Figure 6 shows IR spectra of LiI P(EO)$_n$ polymer electrolytes in the frequency range of 810−890 cm^{-1}. A strong broad band with a maximum at ∼840 cm^{-1} and sharp peak at ∼830 cm^{-1} characterize the IR spectrum of the neat PEO film. The 844 cm^{-1} peak was observed in crystalline PEO.[22] These peaks are assigned to the hybridized vibrations of CH_2 rocking mode and skeletal C−O and C−C stretching, which has all −O−C−C−O− torsional angles in gauche conformations.[22−24] GTTG$^-$ conformation has been widely argued to be of high potential energy and to possess high mobility and weak interchain

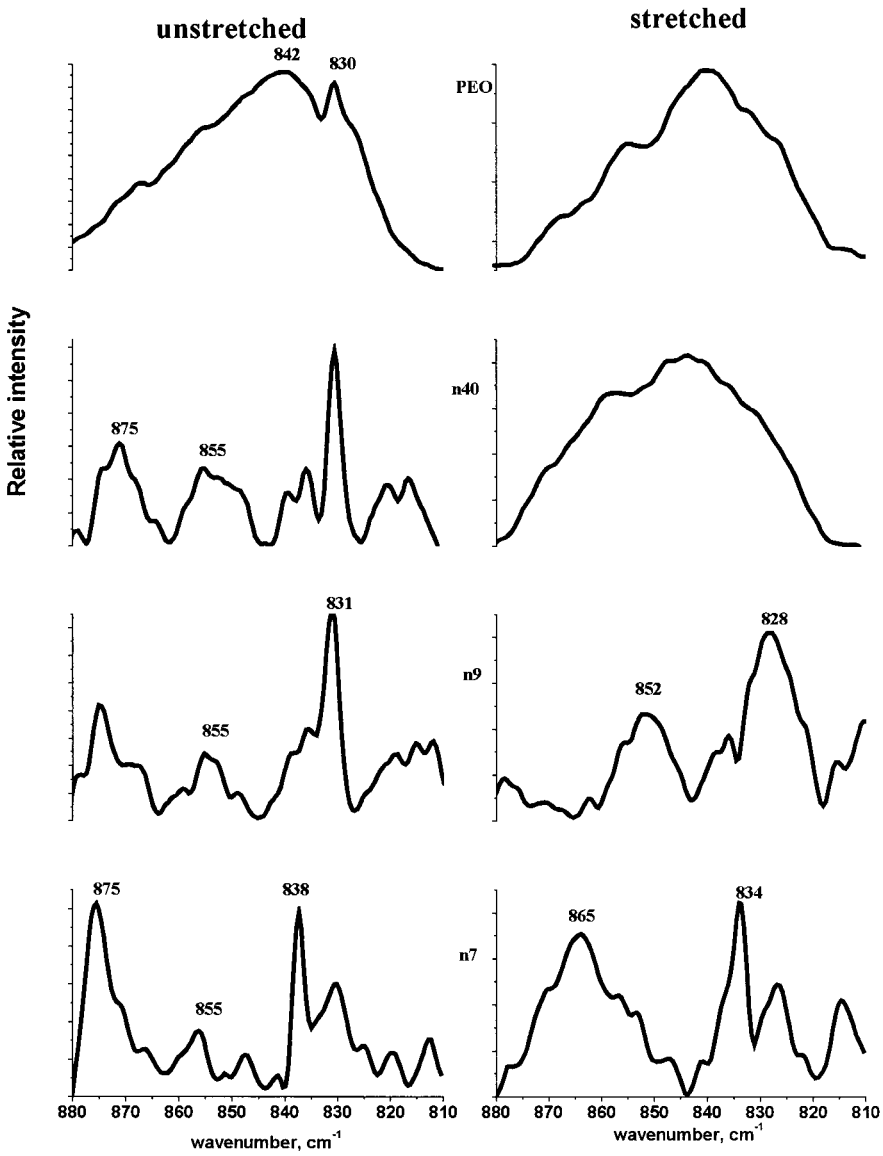

Figure 6. Hybridized vibrations of the CH_2-rocking mode and skeletal C−O and C−C stretch modes.

interaction. The intensity of the 831 cm^{-1} peak, in which the contribution of the CH_2 rocking motions is prevalent, increases with salt concentration up to $n = 9$. The low-intensity shoulder appearing in the 1:40 PE at about 838 cm^{-1} is assigned to C−O stretching mixed with some CH_2 rocking, and gradually grows until it becomes one of the dominant features in the 1:7 LiI P(EO) electrolyte. New concentration-dependent IR conformers are generated at about 855 and 875 cm^{-1}. Studies of PEO−lithium triflate[25] show that the new bands appearing in this region upon the addition of salt originate in the CH_2 rocking vibrations of a chain conformation in which the −O−C−C−O torsional angle is decreased relative to its value in PEO. By analogy, 855 and 875 cm^{-1} bands may be associated with the formation of LiI−PEO complexes. Complex formation, in turn, may cause alter the PEO structure from the extended and open helix of pure PEO to a compressed helix similar to that observed in Na−P(EO) complexes.[23]

The spectra of dilute polymer electrolytes after stretching are almost identical to those of the stretched pure PEO, thus indicating that the stretching affects mainly the polymer phase and not the complex in agreement with the X-ray diffraction data.[21] In the concentrated PEs the effect of stretching on the skeletal stretching vibrations of the C−O and C−C bonds and CH_2 rocking mode is less pronounced. The corresponding peaks, however, become broader, the peak maxima are shifted downward, and the complex-associated bands almost disappear even in the 1:7 stretched polymer electrolyte. This general pattern has been seen also in the region of skeletal deformation vibrations (CCO and COC bending and C−O and C−C torsion) below 600 cm^{-1}.[21] The broadening of the bands and their frequency shift toward low energies, observed on stretching of even concentrated polymer electrolytes, suggest that stretching reverses to some extent the effect of salt addition to the PEO, leading to a restoration of the original extended helix shape. Since the conformational changes in the PEO−LiI complexes are achieved by a change in the torsional O−C−C−O angle, which has a very low rotational energy barrier, it is suggested that the cation in stretched polymer electrolyte can gain an energetically beneficial (as far as transport is concerned) local environment as compared to those in unstretched polymer electrolyte.

Figure 7 shows IR spectra of unstretched PEO and polymer electrolytes in the CH_2 wagging vibrations region. A strong broad band with two clear maxima at ∼1360 and 1340 cm^{-1} and two shoulders is assigned to the asymmetric wagging vibrations of the CH_2 group with respect to the C−C axis of

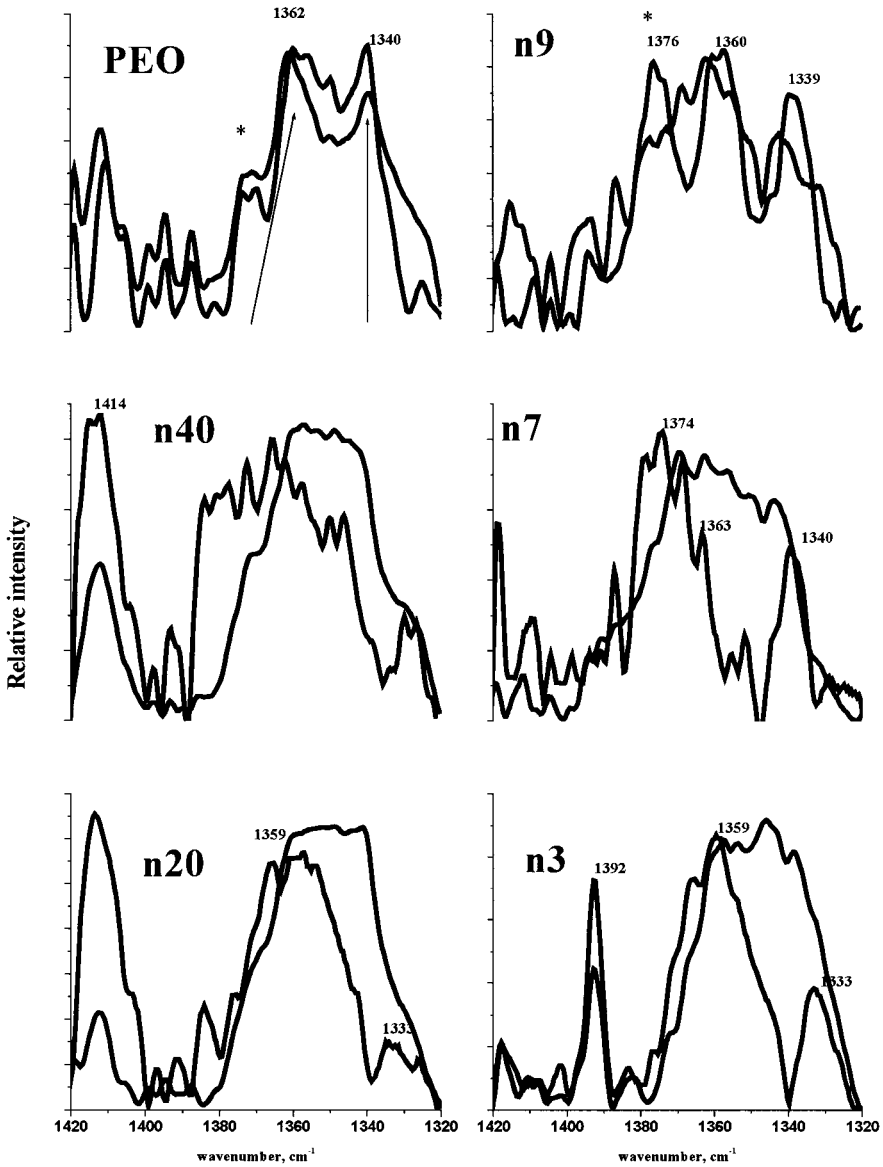

Figure 7. IR spectra in the CH_2-wagging vibration region.

the OCH_2-CH_2O sequence. Upon complexation the intensity of the low-frequency band decreases. The shoulder at 1374 cm^{-1} becomes more resolved with increase in salt concentration, developing into the separate peak at $n = 9$. The peak at ~1412 cm^{-1} is due to the CH_2 symmetric wagging. The intensity of this peak gradually increases with salt addition in dilute polymer electrolytes and becomes dominant at $n = 20$. In concentrated PEs, however, high-energy symmetric vibrations are suppressed, but another narrow strong band at 1393 cm^{-1} prevails in the IR spectrum of the PE with $n = 3$. The most striking change in the CH_2 wagging vibrations region is a pronounced broadening of all the wagging bands. The doublet pattern at ~1360 and 1340 cm^{-1} coalesces into a single broad peak and shifts toward low frequencies as a result of stretching.

The sensitivity of the CH_2-wagging vibrations to the orientation of polymer chains has been discussed previously by Straka and co-workers, who reported that the CH_2 wagging bands at ~1340 and 1362 cm^{-1} correspond to the transition dipole moment orientations parallel and perpendicular with respect to the direction of the chain, respectively.[26] The analysis of the fine structure of the bands showed that their absorbance ratio (A_{1340}/A_{1362}) is about 0.85 for the neat PEO and rubber-like structure PEs with a maximum of 1.05 for LiI $P(EO)_7$. For dilute and concentrated PEs it is about 0.43. On stretching, the A_{1340}/A_{1362} ratio of all the polymer electrolyte samples approaches unity.

Stretching was found to have a similar effect on the width and positions of bands in the region of twisting out-of-plane vibrations of the CH_2 group, whereas the scissoring in-plane deformations of the CH_2 groups are hampered. This effect is more pronounced in the $n = 9$ compound, as shown in Figure 8.

We believe that the observed changes are related to the local conformational changes, favoring CH_2 wagging vibrations. Stretched polymer electrolyte seems to adopt an aligned helical structure, in which the CH_2 groups all face outward. This conformation facilitates wagging and twisting out-of-plane deformations. In the aligned conformation of the helix the oxygen atoms are directed inward, lining the tunnel cavity, and thus favoring cation transport.[27] Previous NMR results obtained in our laboratory showed that the Li^+ local environment of LiI $P(EO)_{20}$ is affected by stretching.[15,16]

We were not able to make any diffusion measurements below 60 °C, due to lack of observed echo attenuation within our gradient strength limits. Figure 9 shows the spectra of stretched LiI $P(EO)_9$ at this temperature in two orientations, parallel and

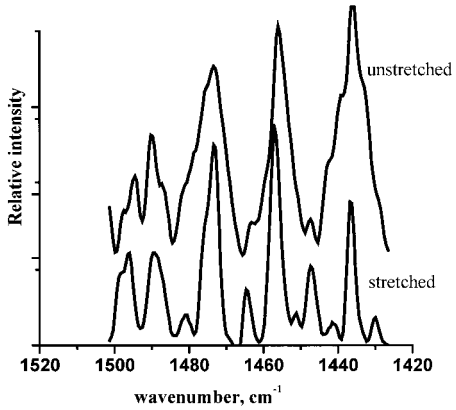

Figure 8. IR spectra in the CH_2 -scissoring vibration region of LiI:$P(EO)_9$ polymer electrolyte.

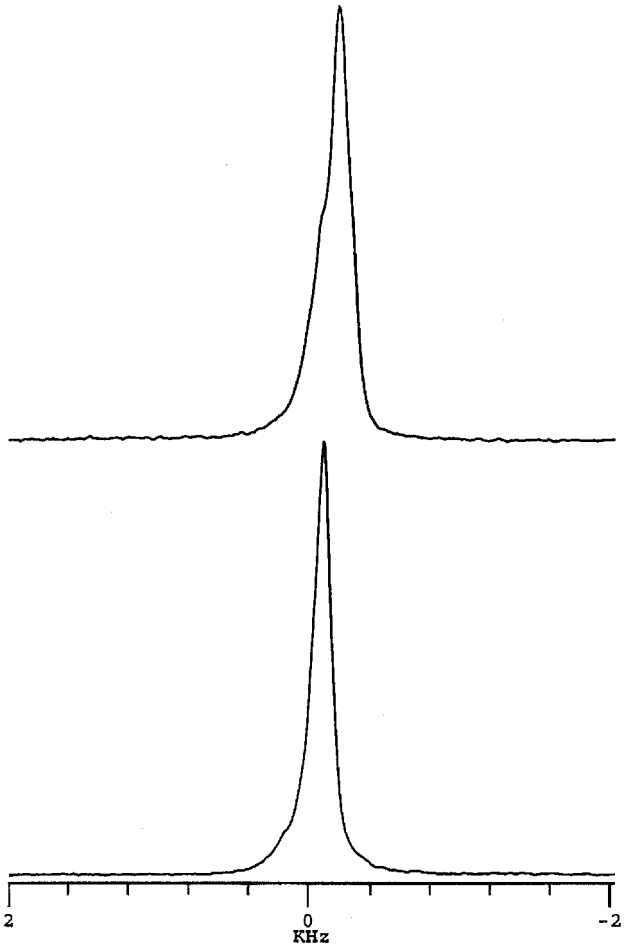

Figure 9. ^{7}Li NMR spectra of stretched PEO_9LiI. Top: magnetic field parallel to stretch axis; bottom: magnetic field perpendicular to stretch axis.

perpendicular to the stretch axis. The observed significant difference in the line widths of the stretched sample at the two orientations clearly indicates anisotropy of the NMR broadening mechanism, which is primarily the heteronuclear ^{7}Li−^{1}H dipolar interaction. Detailed orientation-dependent line widths were reported in a previous study of stretched LiI $P(EO)_{20}$.[15] Table 1 lists the ^{7}Li diffusion coefficients obtained at 60 °C for the unstretched and stretched LiI $P(EO)_9$ samples oriented parallel and perpendicular to the static external magnetic field (which is also the direction of the pulsed field gradient). From the table the anisotropy in the Li^+ ion diffusion can clearly be seen. The diffusion along the stretched direction is almost 4 times greater than in the orthogonal direction. These data support the notion that Li^+ diffusivity is enhanced by alignment of the helical structural units of the polymer and that segmental motion-assisted ion hopping is not the only conduction mechanism. It is interesting to note that value for the unstretched sample at 60 °C lies between the parallel and perpendicular values for the stretched sample. Finally, it is noted that the observed anisotropy is lost after heating the material to 77 °C, and cooling it back to 60 °C. In our previous investigations the relative role of the cations and anions in the enhanced conductivity could not be ascertained.[15,16] However, it is shown here unambiguously via the Li diffusion anisotropy that cation transport is significantly enhanced, although the degree of anion transport enhancement cannot be determined at this time (due to lack of suitable NMR nuclei in the anion).

TABLE 1: ^{7}Li Diffusion Coefficients Obtained at 60 °C for the Unstretched and Stretched LiI $P(EO)_9$ Samples Oriented Parallel and Perpendicular to the Static External Magnetic Field

PEO_9LiI@60 °C	Li^+ diff. coeff. (cm^2/s)
unstretched	7.6×10^{-8}
stretched, ⊥	2.8×10^{-8}
stretched, ∥	1.1×10^{-7}
stretched, ∥ following 77 °C anneal	8.0×10^{-8}

Summary

Microscopy (SEM and AFM) and thermal (DSC) measurements show that stretching results in the formation of an ordered LiI:$P(EO)_n$ polymer electrolyte structure. Unidirectionally oriented fibrous microphases are clearly distinguished in the SEM micrographs. The observed significant changes in the FTIR spectra of the LiI:$P(EO)_n$ electrolytes are attributed to stretching-induced changes in local structure which cause variations in the vibrations of the $-CH_2$ and COC groups. The shifts and the appearance of new bands as a result of increase in salt concentration suggest strong interaction of Li^+ with the oxygen of the $O-CH_2$ group. The stretching of LiI:$P(EO)_n$ electrolytes can be mainly related to the perturbation of the CH_2 groups and −O−C−C−O− torsional angles. We believe that stretched polymer adopts a modified helical structure, similar to that of an extended salt-free PEO helix. In this conformation the CH_2 groups all face outward. This facilitates wagging and twisting out-of-plane deformations. In the aligned conformation of the helix the oxygen atoms are directed inward, lining the tunnel cavity, thus favoring cation transport. The stretching process was found to influence the DC conductivity in the direction of the applied force more strongly than does an increase in temperature (from 28° to 60 °C). The stretching-induced longitudinal conductivity enhancement and low apparent activation energy found in more ordered polymer electrolyte hosts are attributed to fast cation migration within the helical channels. This conclusion is strongly supported by the observed Li NMR diffusion anisotropy. The maximum conductivity enhancement (about 40-fold) in the stretch direction found at $n = 7$, is attributed to highly aligned cylindrical tunnels for Li^+ transport in double PEO chains coordinating the cations, as suggested by ref 13. It is likely that anion transport outside along the helical direction can also play a role in the enhanced conductivity, but NMR diffusion measurements on more suitable anions (e.g., containing fluorine) are necessary to demonstrate this conclusively.

Acknowledgment. We thank Prof. A. Nitzan of Tel Aviv University for useful discussions on stretched polymer systems.

This work was supported by Israel Academy of Science, the U.S. Department of Energy, and the U.S. Office of Naval Research.

References and Notes

(1) *Polymer Electrolyte Review I*; MacCallum, J. R., Vincent, C. A., Eds.; Elsevier Applied Science: London, 1989.

(2) *Polymer Electrolyte Review II*; MacCallum, J. R, Vincent, C. A., Eds.; Elsevier Applied Science: London, 1989.

(3) Armand, B. M. *Annu. Rev. Mater. Sci.* **1986**, *16*, 245−261.

(4) Gray, F. M. *Solid Polymer Electrolytes*; VCA, 1991.

(5) Kumar, B.; Scanlon, L. G. *Power Sources, J.* **1994**, *52*, 261−268.

(6) Ratner, M. A. *Polymer Electrolyte Review I*; MacCallum, J. R., Vincent, C. A., Eds.; Elsevier Applied Science Publishers: London, 1987.

(7) Druger, S. D.; Ratner, M. A.; Nitzan, A. *Solid State Ionics* **1983**, *9/10*, 1115−1120.

(8) *Solid State Electrochemistry*; Bruce, P. G., Ed; Cambridge University Press: New York, 1995.

(9) Gray, F.; Armand, M. *Polymer Electrolytes in Handbook of Battery Materials*; Besenhard, J. O., Ed.; Wiley-VCH: New York, 1999; pp 499−520.

(10) Robitaille, C. D.; Fauteax, D. *J. Electrochem Soc*. **1986**, *133*, 315.

(11) Papke, B. L.; Ratner, M. A.; Shriver, D. F. *J. Phys. Chem. Solids* **1986**, *42*, 493−500.

(12) Armand, M. B.; Chabagno, J. M.; Duclot, M. In *Fast Ion Transport in Solids*; Vashishta, P., Mundy, J. N., Shenoy, G. K., Eds.; North-Holland, New York, 1979; p 131.

(13) MacGlashan, G. S.; Andreev, Y. G.; Bruce, P. *Nature* **1999**, *398*, 792−794.

(14) Golodnitsky, D.; Peled, E. *Electrochim. Acta* **2000**, *45*, 1431−1436.

(15) Chung, S. H.; Wang, Y.; Greenbaum, S. G.; Golodnitsky, D.; Peled, E. *Electrochem. Solid-State Lett.* **1999**, *2*, 553−555.

(16) Golodnitsky, D.; Peled, E.; Livshits, E.; Rozenberg, Yu.; Chung, S. H.; Wang, Y.; Greenbaum, S. *J. Electroanal. Chem.* **2000**, *491*, 203-210.

(17) Hille, B. *Ionic channels of excitable membranes*, 2nd ed.; Sunderland, Sinauer, 1992; p 607.

(18) Tanigawara, Y.; Okamura, N.; Hirai, M.; Yasuhara, M.; Ueda, K.; Kioka, N.; Komano, T.; Hori, R. *J. Pharmacol. Exp. Ther*. **1992**, *263*, 840−845.

(19) Golodnitsky, D.; Ardel, G.; Strauss, E.; Peled, E.; Lareah, Y.; Rosenberg, Yu. *J. Electrochem. Soc.* **1997**, *144*, 3484−3491.

(20) Chung, S. H.; Bajue, S.; Greenbaum, S. G. *J. Chem. Phys.* **2000**, *112*, 8515.

(21) Golodnitsky, D.; Livshits, E.; Lapides, I.; Rosenberg, Yu.; Peled, E. *Solid State Ionics*, submitted.

(22) Matsuuda, H.; Fukuhara, K. *J. Polym. Sci.: Part B: Polym. Phys.* **1986**, *24*, 1383−1400.

(23) Rhodes, C. P.; Frech, R. *Solid State Ionics* **1999**, *121*, 91−99.

(24) Papke, B. L.; Ratner, M. A.; Shriver, D. F. *J. Phys. Chem. Solids* **1981**, *42*, 493−500.

(25) Frech, R.; Huang, W. *Macromolecules* **1995**, *28*, 1246−1251.

(26) Straka, J.; Schmidt, P.; Dybal, J.; Schneider, B.; Spevacek, J. *Polymer* **1995**, *36*, 1147−1155.

(27) Ratner, M.; Johanson, P.; Shriver, D. F. *Mater. Res. Soc. Bull.* **2000**, *3*, 31−37.